

# AFM imaging with an *xy*-micropositioner with integrated tip

P.-F. Indermühle<sup>a,\*</sup>, V.P. Jaecklin<sup>a</sup>, J. Brugger<sup>a</sup>, C. Linder<sup>a</sup>, N.F. de Rooij<sup>a</sup>,  
M. Binggeli<sup>b</sup>

<sup>a</sup> *IMT, University of Neuchâtel, Breguet 2, CH-2000 Neuchâtel, Switzerland*

<sup>b</sup> *Swiss Center for Electronics and Microtechnology Inc. (CSEM), Maladière 71, CH-2000 Neuchâtel, Switzerland*

## Abstract

We have fabricated an *xy*-microstage with integrated protruding tip and electrostatic comb actuators for scanning probe surface imaging. This device, which is micromachined in monocrystalline silicon, has been actuated and characterized and, for the first time with such a microtool, an atomic force microscope (AFM) profile has been achieved.

*Keywords:* Atomic force microscopy; *xy*-Micropositioner

## 1. Introduction

The invention of the scanning tunnelling microscope (STM) and of the atomic force microscope (AFM) opened new perspectives in surface analysis [1,2], while the realization of such devices defined new challenges for microengineering [3,4].

We have constructed an *xy*-microstage with an integrated sharp tip for AFM profiling, electrostatic comb actuators for lateral displacement and a via hole for optical detection [5]. This device, micromachined in monocrystalline silicon, does not need manual assembly of the discrete components (protruding tip on a smooth beam driven by piezoelectric elements). Further, the thermal and vibrational noise level should be reduced by miniaturization.

In this paper, we first present an improved fabrication sequence for this structure. Then, its operation is described, with special attention to the first AFM profile realized with such a device. Finally, results are briefly discussed.

## 2. Improved fabrication sequence

Three modifications have been made to the process already published [5].

First, the silicon dioxide (SiO<sub>2</sub>) layer grown on the upper wafer is only 0.1 instead of 1 μm thick. This

reduces the SiO<sub>2</sub> underetching and allows a better resolution of the initial pattern (Fig. 1). Secondly, a 10–15 μm deep groove is etched under the movable part of the structures during the second step. Thus, the stress in the 1 μm thick SiO<sub>2</sub> layer of the lower wafer does not break the device when it is being released. This groove also reduces the sticking of the free-standing structure to the substrate, allows higher voltages to be applied on the comb actuators and makes the positioning of the optical fibre as well as the approach of the sample easier. Thirdly, only dry etching is performed for defining the tip. Better homogeneity in beam and suspension dimensions is thus obtained and, moreover, the tip curvature radius is reduced (the best tips have a radius of less than 10 nm). Figs. 2 and 3 illustrate the improved structure.

## 3. Operation and characterization

The measured lateral displacement versus applied voltage of a structure whose beams and suspensions were about 2 μm wide and 3 μm thick is shown in Fig. 4. It has been obtained by applying a d.c. voltage ranging from 0 to 200 V on one comb actuator and by visually measuring the displacement on the screen of a video camera connected to a microscope. The accuracy of the measurement is ±0.5 μm. As expected, the curve shows a good second-order fitting [6]. A maximum displacement of 12 μm has been observed with an applied voltage of 300 V.

\* Corresponding author.

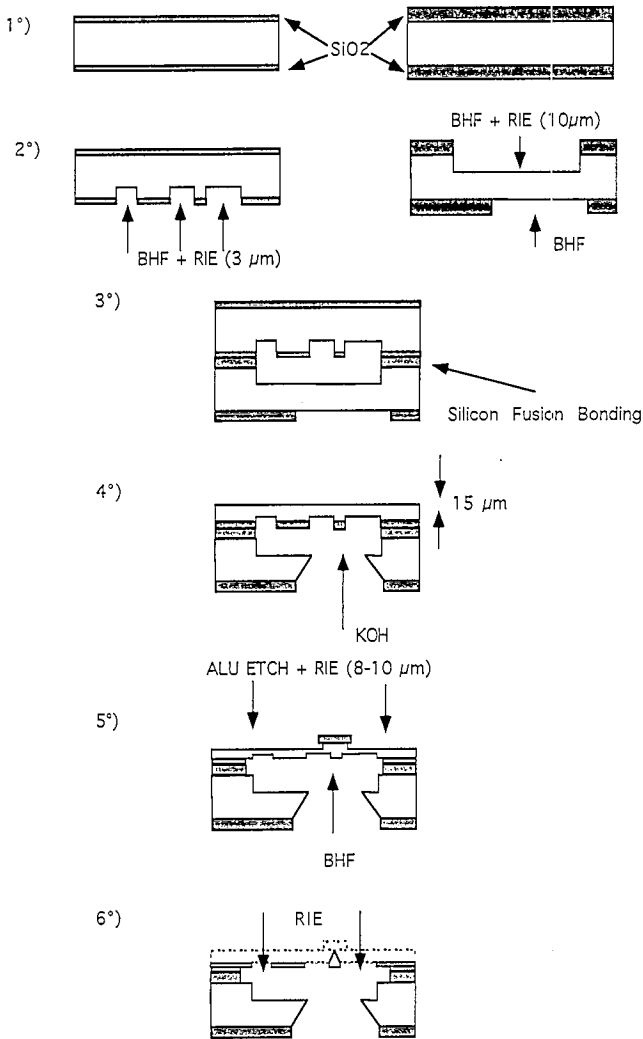


Fig. 1. Detailed fabrication process of the improved overhanging *xy*-microstage: (1) thermal oxidation (0.1 and 1  $\mu\text{m}$  layer) of a pair of silicon wafers; (2) photolithography and BHF etching for patterning the  $\text{SiO}_2$  of the lower side of both wafers and upper side of lower wafer, reactive ion etching (RIE,  $\text{C}_2\text{F}_6/\text{SF}_6$ ) for prestructuring of the upper wafer and groove etching on the lower wafer; (3) aligned prebonding followed by fusion bonding; (4) etching of the via holes (lower wafer) and thinning of the upper wafer in KOH solution; (5) etching of the interface oxide layer where it is accessible through the via holes; metallization and metal patterning; RIE on the upper side to form the columns for the tips; (6) final RIE etching to pierce the membrane and form the sharp tip.

The same set-up has been used to determine lateral resonance frequencies. A square signal with an amplitude varying between 0 and 100 V and frequencies ranging from 0 to 30 kHz has been applied to the comb. The first resonance frequency has been observed at about 16 kHz. It has not been possible to determine other lateral modes.

To determine the vertical modes, we glued the structure on a piezoelectric element and measured its response to excitation frequencies between 0 and 20 kHz. Measurements have been carried out with a confocal microscope and with an interferometer in air and in

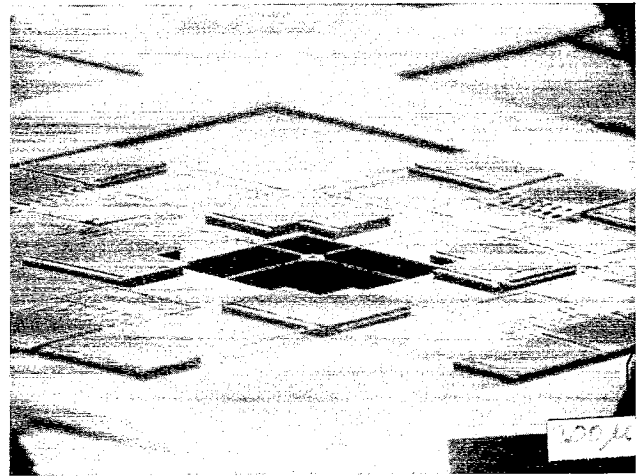


Fig. 2. Top view (SEM) of the improved microfabricated silicon *xy*-microstage.

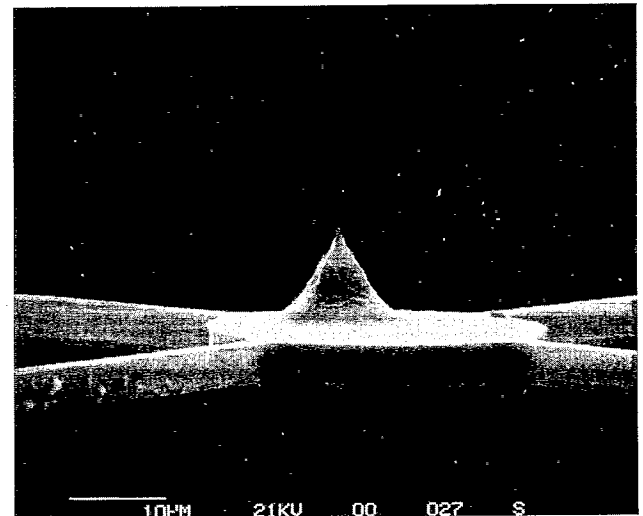


Fig. 3. Close-up view (SEM) of a protruding silicon tip (height 8  $\mu\text{m}$ , radius 80 nm) integrated on the centre table.

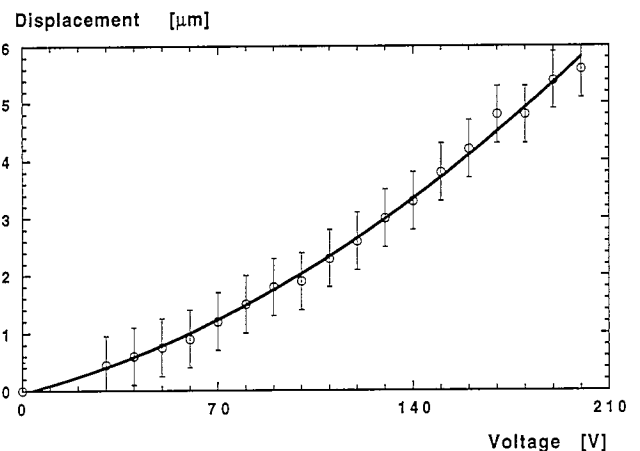


Fig. 4. Displacement vs. applied voltage of a monocrystalline *xy*-micropositioner with integrated tip and via hole for optical detection.

vacuum. A first resonance frequency has been found at about 13 kHz.

Finally, the integrated microstage has been fitted into a commercial instrument and, for the first time, an AFM image has been obtained by means of such an integrated structure (Fig. 5). Imaging has been carried out in contact mode on the side of a tungsten carbide needle without a feedback loop (Fig. 6). The image is in good agreement with another profile realized on the same sample with a commercial instrument (Fig. 7).

#### 4. Discussion

The higher noise on the image realized with the integrated microstage may be explained by the set-up we used. Since the electrical contacts of the comb actuators are located on the same level as the tip, a relatively long and fine sample was necessary. We glued a microprober needle on a home-made positioning set-up which, because of observation and electrical contact requirements, was not as stable as a standard AFM sample holder.

The non-linearity of the displacement as a function of the applied voltage (Fig. 4) induces a distortion of the picture. However, since the quadratic coefficient is small (about  $10^{-5}$ ) and the dimensions of the scanned area do not exceed  $1 \mu\text{m} \times 1 \mu\text{m}$ , Fig. 5 shows the image without distortion corrections.

The horizontal scale has been approximated by knowing the applied scanning voltage (Fig. 4). This estimation was in good agreement with the scale of the profile realized with the commercial AFM.

#### 5. Conclusions

We have fabricated and operated an *xy*-microstage with integrated comb actuators for scanning displacement, a sharp tip for AFM profiling and a via hole for optical detection, which has been entirely micro-machined in monocrystalline silicon. A lateral displacement versus applied voltage curve has been measured, which indicates that the microstage can be moved over an area of about  $3 \mu\text{m} \times 3 \mu\text{m}$  by actuating two combs with voltages of 150 V. First resonance frequencies of the structure have been measured and values higher than 10 kHz, and thus beyond the environmental noise, have been found.

Using such an integrated prototype structure, an AFM profile has been realized. It is in good agreement with another AFM image of the same sample obtained with a commercial instrument.

Further improvements like backside electrical contacts and integrated optics are planned in order to build a real stand-alone AFM microtool.

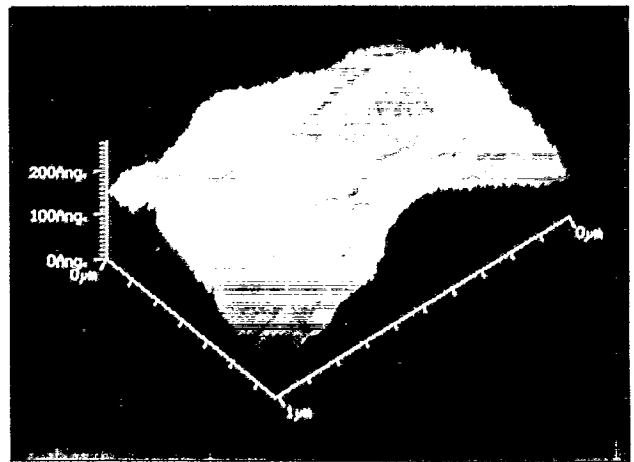


Fig. 5. AFM image realized with the prototype *xy*-microstage.

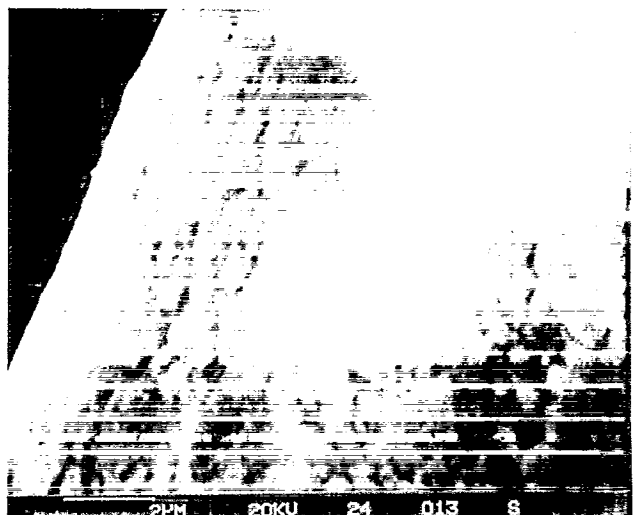


Fig. 6. SEM micrograph of the sample (tungsten carbide needle).

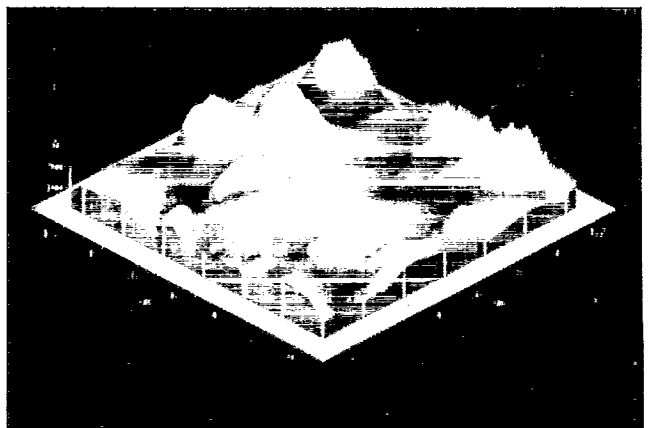


Fig. 7. AFM image obtained with a commercial instrument.

#### Acknowledgements

We are grateful to the whole staff of the IMT and CSEM for scientific and technical assistance. This work

was supported by the Swiss National Science Foundation and the Swiss Foundation for Microtechnology Research.

## References

- [1] G. Binnig, H. Rohrer, Ch. Gerber and E. Weibel, Surface studies by scanning tunneling microscopy, *Phys. Rev. Lett.*, 49 (1982) 57.
- [2] G. Binnig, C.F. Quate and Ch. Gerber, Atomic force microscope, *Phys. Rev. Lett.*, 56 (1986) 930.
- [3] N.C. MacDonald, Nanomechanisms and tips for microinstruments, *Proc. 7th Int. Conf. Solid-State Sensors and Actuators (Transducers '93)*, Yokohama, Japan, June 7-10, 1993, p. 8.
- [4] J. Brugger, R.A. Buser and N.F. de Rooij, Silicon cantilevers and tips for scanning force microscopy, *Sensors and Actuators A*, 34 (1992) 193.
- [5] P.-F. Indermühle, C. Linder, J. Brugger, V.P. Jaecklin and N.F. de Rooij, Design and fabrication of an overhanging *xy*-microactuator with integrated tip for scanning surface profiling, *Sensors and Actuators A*, 43 (1994) 346.
- [6] V.P. Jaecklin, C. Linder, N.F. de Rooij and J.M. Moret, Micromechanical comb actuators with low driving voltage, *J. Micromech. Microeng.*, 2 (1992) 250.